hp–Discontinuous Galerkin Finite Element Methods with Least–Squares Stabilization

Paul Houston[1], Max Jensen[2] and Endre Süli[2]

Abstract. We consider a family of *hp*–version discontinuous Galerkin finite element methods with least–squares stabilization for symmetric systems of first-order partial differential equations. The family includes the classical discontinuous Galerkin finite element method, with and without streamline–diffusion stabilization, as well as the discontinuous version of the Galerkin least–squares finite element method. An *hp*–optimal error bound is derived in the associated DG–norm. If the solution of the problem is elementwise analytic, an exponential rate of convergence under *p*–refinement is proved. We perform numerical experiments both to illustrate the theoretical results and to compare the various methods within the family.

Keywords. *hp*–finite element methods, discontinuous Galerkin methods, least-squares finite element methods, first order systems of PDEs

AMS subject classifications. 65N12, 65N15, 65N30

1 Introduction

First-order systems of partial differential equations arise in a number of physical applications and their numerical solution is of great practical interest. Unfortunately, the standard Galerkin finite element approximation of a first-order partial differential equation based on *continuous* piecewise polynomials (CGFEM) exhibits poor stability properties which manifest themselves as large nonphysical numerical oscillations whose frequency is commensurable with the mesh size.

Over the last two decades considerable progress has been made in the area of stabilized finite element methods for the numerical solution of first-order hyperbolic problems and second-order partial differential equations with dominant hyperbolic behavior; a particularly significant method from this class is the streamline–diffusion finite element method of Hughes and Brooks [12] which incorporates numerical dissipation in the characteristic (or streamwise) direction with the aim to suppress the undesirable numerical oscillations in the standard continuous Galerkin finite element method. A rigorous error analysis of this technique was performed by

[1]Department of Mathematics & Computer Science, University of Leicester, Leicester LE1 7RH, UK (e-mail: Paul.Houston@mcs.le.ac.uk).

[2]Oxford University Computing Laboratory, Wolfson Building, Parks Road, Oxford OX1 3QD, UK (e-mails: Max.Jensen@comlab.ox.ac.uk and endre@comlab.ox.ac.uk).

Johnson, Nävert and Pitkäranta [13]. More recently, the hp–version of the streamline–diffusion finite element method for first-order hyperbolic problems and second-order partial differential equations with nonnegative characteristic form was considered by Houston, Schwab and Süli [9] and Houston and Süli [11]; error bounds have been derived which, in the hyperbolic case, are simultaneously optimal with respect to the local mesh size h and the local polynomial degree p, with the local streamline–diffusion parameter δ chosen to be of size h/p.

Another class of methods for first-order hyperbolic equations, based on *discontinuous* piecewise polynomial approximation, was proposed in an early paper of Reed and Hill [17]. The technique is commonly referred to in the literature as the discontinuous Galerkin finite element method (DGFEM). A rigorous error analysis of the method was carried out in a series of papers by Lesaint and Raviart [15], Johnson and Pitkäranta [14] and Richter [16] for linear partial differential equations. For nonlinear hyperbolic problems, the DGFEM was successfully analyzed and implemented by Cockburn and Shu [3, 4, 5, 6, 7]. The hp-version of the discontinuous Galerkin finite element method, with streamline–diffusion stabilization parameter δ of size h/p^2, was proposed and studied by Bey and Oden [1]; they derived an h-optimal but p-suboptimal bound on the global error of the method in the DG-norm. Recently, Houston, Schwab and Süli showed in [9, 19, 20] that with δ of size h/p the method achieves an hp–optimal error bound in the DG-norm. It was also shown that if the solution to the underlying differential equation is elementwise analytic, then the method exhibits an exponential rate of convergence under p-refinement. Subsequently, by using a completely different error analysis, Houston, Schwab and Süli also proved in [10] that the hp–optimality of the method in the DG-norm persists even when the streamline–diffusion parameter is set to zero. This is in sharp contrast with the poor accuracy and stability properties exhibited by the CGFEM for first–order hyperbolic problems in the absence of streamline–diffusion stabilization. The source of this difference between CGFEM and DGFEM is that the interelement jump terms in DGFEM introduce at least as much numerical dissipation as streamline–diffusion stabilization does, and therefore the inclusion of the latter into DGFEM becomes unnecessary. An analogous remark applies when Galerkin least–squares stabilization is used instead of streamline–diffusion stabilization.

While the streamline–diffusion finite element method (with continuous piecewise polynomials) and the discontinuous Galerkin finite element method (both with and without streamline–diffusion or least–squares stabilization) are stable and accurate numerical techniques, when applied to first–order systems of partial differential equations they lead to nonsymmetric systems of linear algebraic equations, even if the system of partial differential equations is symmetric. To rectify this, it is therefore appealing to consider least–squares finite element methods based on discontinuous piecewise polynomials (LS-DGFEM). For a detailed survey of the theory of *continuous* least–squares finite element methods we refer to the review article of Bochev and Gunzburger [2]. It will be shown here that the hp–version LS-DGFEM exhibits the same hp–optimal convergence rate in the associated DG-norm as the hp–version of the (continuous) streamline–diffusion finite element method and the discontinuous Galerkin finite element method (with or without streamline–diffusion or least–squares stabilization). LS-DGFEM leads to a system of linear algebraic equations with a symmetric positive definite matrix, thus enabling the use of standard and robust iterative algorithms such as a preconditioned conjugate gradient method. However, LS-DGFEM is not without disadvantages: even though its formal rate of convergence is identical to that of the streamline–diffusion finite element method with continuous piecewise polynomials and the discontinuous Galerkin finite element method with or without streamline–diffusion or least–squares stabilization, our numerical experiments indicate that LS-DGFEM is more dissipative than either of the above methods. Indeed, the experiments reveal that the excess numerical dissipation in LS-DGFEM is due to the inclusion of least–squares stabilization into the interelement jump terms rather than to the presence of least–squares stabilization in the element integral terms; this finding is consistent with the remark made at the end of the previous paragraph that the dominant source of numerical dissipation in DGFEM are the interelement jump terms.

Despite LS-DGFEM's inferiority in terms of practically observed accuracy when compared with DGFEM, the combination of the two methods has a helpful property: through the inclusion of least-squares stabilization into the interelement jump terms the *local* numerical dissipation of the resulting method can be both *increased* and *decreased* beyond that of DGFEM; as we have already indicated above, the amount of numerical dissipation in DGFEM cannot be controlled in a similar manner through the inclusion of streamline–diffusion stabilization as, at best, this has little or no effect or, worse, it makes the DGFEM more dissipative. The chief purpose of this paper is to investigate this particular mix of DGFEM and LS-DGFEM through embedding the two methods into a one-parameter family of discontinuous Galerkin finite element discretizations.

The structure of the paper is as follows. In the next section we formulate our model problem: a symmetric system of first–order partial differential equations. We then state the hp–version LS-DGFEM discretization of this model problem. In Section 3 we discuss the error analysis of the method and prove that it exhibits hp–optimal convergence in the associated DG-norm; we also show that if the solution is elementwise analytic, then the convergence rate of the method is exponential under p–refinement. In Section 4 we verify our theoretical results through numerical experiments; we also demonstrate that LS-DGFEM suffers from excessive numerical dissipation, and we identify least-squares stabilization in the interelement jump terms as the source of this undesirable feature. The findings of Section 4 lead us to consider in Section 5 a general family of discontinuous Galerkin finite element discretizations which admit completely irregular meshes with an arbitrary number of hanging nodes, and local and componentwise variation of the polynomial degree in the finite element approximation. The family includes DGFEM, with or without least–squares stabilization, as well as LS-DGFEM. We show that the family exhibits *hp*–optimal convergence rates in the associated DG-norm; again, when the solution is elementwise analytic the convergence rate is exponential under p-refinement. We conclude, in Section 6 with numerical experiments which demonstrate the performance of the various schemes.

2 Model problem and the *hp*–LS-DGFEM

Let Ω be a bounded open polyhedral domain in $\mathbb{R}^d$, $d \geq 2$, and let Γ denote the union of open faces of Ω. Suppose that $\mathbf{B} = (\mathbf{B}_1, \ldots, \mathbf{B}_d)$ is a d–component matrix function defined on $\bar{\Omega}$ with $\mathbf{B}_i \in [W^1_\infty(\Omega)]^{m\times m}_{\mathrm{symm}}$, $i = 1, \ldots, d$. Let $\boldsymbol{\mu} = (\mu_1, \ldots, \mu_d)$ denote the unit outward normal vector to Γ, and consider the symmetric matrix $\mathbf{B}(\boldsymbol{\mu}) \equiv \mathbf{B}\cdot\boldsymbol{\mu} = \boldsymbol{\mu}_1\mathbf{B}_1 + \ldots + \boldsymbol{\mu}_d\mathbf{B}_d$. Suppose that $\mathbf{B}$ is diagonalized via $\mathbf{B}(\boldsymbol{\mu}) = X(\boldsymbol{\mu})^{-1}\Lambda(\boldsymbol{\mu})X(\boldsymbol{\mu})$, where $\Lambda(\boldsymbol{\mu})$ is a diagonal matrix, with the (real) eigenvalues of $\mathbf{B}(\boldsymbol{\mu})$ appearing along its diagonal. We shall suppose that Γ is nowhere characteristic in the sense that none of the diagonal entries of $\Lambda(\boldsymbol{\mu})$ is zero for any choice of the unit outward normal vector $\boldsymbol{\mu}$ on Γ. We decompose $\Lambda(\boldsymbol{\mu})$ as $\Lambda(\boldsymbol{\mu}) = \Lambda_-(\boldsymbol{\mu}) + \Lambda_+(\boldsymbol{\mu})$, where $\Lambda_-(\boldsymbol{\mu})$ is diagonal and negative semidefinite, and $\Lambda_+(\boldsymbol{\mu})$ is diagonal and positive semidefinite. Thus we define

$$\mathbf{B}_-(\boldsymbol{\mu}) = X(\boldsymbol{\mu})^{-1}\Lambda_-(\boldsymbol{\mu})X(\boldsymbol{\mu}) \quad \text{and} \quad \mathbf{B}_+(\boldsymbol{\mu}) = X(\boldsymbol{\mu})^{-1}\Lambda_+(\boldsymbol{\mu})X(\boldsymbol{\mu}).$$

Clearly, for each $\boldsymbol{\mu}$ on Γ, $\mathbf{B}(\boldsymbol{\mu}) = \mathbf{B}_-(\boldsymbol{\mu}) + \mathbf{B}_+(\boldsymbol{\mu})$.

Given $\mathbf{C} \in [L_\infty(\Omega)]^{m\times m}$, $\mathbf{f} \in [L_2(\Omega)]^m$ and $\mathbf{g} \in [L_2(\Gamma)]^m$, we consider the following boundary value problem: find $\mathbf{u} \in H(\mathcal{L}, \Omega)$ such that

$$\mathcal{L}\mathbf{u} \equiv \nabla\cdot(\mathbf{B}\mathbf{u}) + \mathbf{C}\mathbf{u} = \mathbf{f} \quad \text{in } \Omega\,, \qquad \mathbf{B}_-(\boldsymbol{\mu})\mathbf{u} = \mathbf{B}_-(\boldsymbol{\mu})\mathbf{g} \quad \text{on } \Gamma\,, \tag{2.1}$$

where $H(\mathcal{L}, \Omega) = \{\mathbf{v} \in [L_2(\Omega)]^m : \mathcal{L}\mathbf{v} \in [L_2(\Omega)]^m\}$ denotes the *graph space* of the partial differential operator $\mathcal{L}$ in $L_2(\Omega)$. Next, we formulate the *hp*–version of the least–squares Discontinuous Galerkin Finite Element Method (*hp*–LS-DGFEM, for short) for the numerical solution of (2.1).

Suppose that $k \geq 1$, and $\mathcal{T}_h$ is a regular or k–irregular subdivision of Ω into disjoint open element domains κ such that $\bar{\Omega} = \cup_{\kappa\in\mathcal{T}_h}\bar{\kappa}$. Thus a

$(d-1)$-dimensional face of each element κ in $\mathcal{T}_h$ is allowed to contain at most k hanging (irregular) nodes; when $k=1$, the hanging node is typically the barycenter of the face. We shall suppose that the family of subdivisions $\mathcal{T}_h$ is shape–regular and that each $\kappa \in \mathcal{T}_h$ is a smooth bijective image of a fixed master element $\hat{\kappa}$, that is, $\kappa = F_\kappa(\hat{\kappa})$ for all $\kappa \in \mathcal{T}_h$, where $\hat{\kappa}$ is either the open unit simplex or the open unit hypercube $(-1,1)^d$ in $\mathbb{R}^d$. On the reference element $\hat{\kappa}$, with $\hat{\mathbf{x}} = (\hat{x}_1, \dots, \hat{x}_d) \in \hat{\kappa}$ and $\boldsymbol{\alpha} = (\alpha_1, \dots, \alpha_d) \in \mathbb{N}_0^d$, we define spaces of polynomials of degree $p \geq 1$ as follows:

$$\mathcal{Q}_p = \operatorname{span}\{\hat{\mathbf{x}}^{\boldsymbol{\alpha}} : 0 \leq \alpha_i \leq p,\ \ 1 \leq i \leq d\}, \quad \mathcal{P}_p = \operatorname{span}\{\hat{\mathbf{x}}^{\boldsymbol{\alpha}} : 0 \leq |\alpha| \leq p\}.$$

To each $\kappa \in \mathcal{T}_h$ we assign an integer $p_\kappa \geq 1$; collecting the p_κ and F_κ in the vectors $\mathbf{p} = \{p_\kappa : \kappa \in \mathcal{T}_h\}$ and $\mathbf{F} = \{F_\kappa : \kappa \in \mathcal{T}_h\}$, respectively, we introduce the finite element space

$$\begin{aligned} S^{\mathbf{p}}(\Omega, \mathcal{T}_h, \mathbf{F}) \ = \ \{\mathbf{v} \in [L_2(\Omega)]^m \ : \ &\mathbf{v}|_\kappa \circ F_\kappa \in [\mathcal{Q}_{p_\kappa}]^m \text{ if } F_\kappa^{-1}(\kappa) = (-1,1)^d, \\ &\text{and } \mathbf{v}|_\kappa \circ F_\kappa \in [\mathcal{P}_{p_\kappa}]^m \text{ if } F_\kappa^{-1}(\kappa) \text{ is the open unit simplex; } \kappa \in \mathcal{T}_h\}. \end{aligned}$$

Given that $\mathcal{T}_h$ is a subdivision of Ω, we define the broken Sobolev space $H^{\mathbf{s}}(\Omega, \mathcal{T}_h)$ of composite index $\mathbf{s}$ with nonnegative components s_κ, $\kappa \in \mathcal{T}_h$, by

$$[H^{\mathbf{s}}(\Omega, \mathcal{T}_h)]^m = \{\mathbf{v} \in [L_2(\Omega)]^m : \ \mathbf{v}|_\kappa \in [H^{s_\kappa}(\kappa)]^m \quad \forall \kappa \in \mathcal{T}_h\}.$$

If $s_\kappa = s \geq 0$ for all $\kappa \in \mathcal{T}_h$, we shall simply write $[H^s(\Omega, \mathcal{T}_h)]^m$.

Given that κ is an element in the subdivision $\mathcal{T}_h$, we denote by $\partial\kappa$ the union of $(d-1)$-dimensional open faces of κ. Let $\mathbf{x} \in \partial\kappa$ and suppose that $\mathbf{n}_\kappa(\mathbf{x})$ denotes the unit outward normal vector to $\partial\kappa$ at $\mathbf{x}$. With these conventions, we define $\mathbf{B}(\mathbf{n}_\kappa)$, $\mathbf{B}_-(\mathbf{n}_\kappa)$ and $\mathbf{B}_+(\mathbf{n}_\kappa)$ analogously to $\mathbf{B}(\boldsymbol{\mu})$, $\mathbf{B}_-(\boldsymbol{\mu})$ and $\mathbf{B}_+(\boldsymbol{\mu})$ above, respectively. For each $\kappa \in \mathcal{T}_h$ and any $\mathbf{v} \in [H^1(\kappa)]^m$ we denote by $\mathbf{v}_\kappa^+$ the interior trace of $\mathbf{v}$ on $\partial\kappa$ (the trace taken from within κ). Now consider an element κ such that the set $\partial\kappa\backslash\Gamma$ is nonempty; then for each $\mathbf{x} \in \partial\kappa\backslash\Gamma$ (with the exception of a set of $(d-1)$–dimensional measure zero) there exists a unique element κ', depending on the choice of $\mathbf{x}$, such that $\mathbf{x} \in \partial\kappa'$. Suppose that $\mathbf{v} \in [H^1(\Omega, \mathcal{T})]^m$. If $\partial\kappa\backslash\Gamma$ is nonempty for some $\kappa \in \mathcal{T}_h$, then we define the outer trace $\mathbf{v}_\kappa^-$ of $\mathbf{v}$ on $\partial\kappa\backslash\Gamma$ relative to κ as the inner trace $\mathbf{v}_{\kappa'}^+$ relative to those elements κ' for which $\partial\kappa'$ has intersection with $\partial\kappa\backslash\Gamma$ of positive $(d-1)$–dimensional measure. We also introduce the jump of $\mathbf{v}$ across $\partial_-\kappa\backslash\Gamma_-$: $[\mathbf{v}]_\kappa = \mathbf{v}_\kappa^+ - \mathbf{v}_\kappa^-$. Since below it will always be clear from the context which element κ in the subdivision $\mathcal{T}_h$ the quantities $\mathbf{n}_\kappa$, $\mathbf{v}_\kappa^+$, $\mathbf{v}_\kappa^-$ and $[\mathbf{v}]_\kappa$ correspond to, for the sake of notational simplicity we shall suppress the letter κ in the subscript and write, respectively, $\mathbf{n}$, $\mathbf{v}^+$, $\mathbf{v}^-$ and $[\mathbf{v}]$ instead.

For $\mathbf{v}, \mathbf{w} \in [H^1(\Omega, \mathcal{T}_h)]^m$, we introduce the bilinear form

$$B_{\mathrm{LS}}(\mathbf{w}, \mathbf{v}) = \sum_{\kappa \in \mathcal{T}_h} \frac{h_\kappa}{p_\kappa} \int_\kappa \mathcal{L}\mathbf{w} \cdot \mathbf{M}_\kappa \mathcal{L}\mathbf{v} \ \mathrm{d}x + \sum_{\kappa \in \mathcal{T}_h} \int_{\partial\kappa\backslash\Gamma} \mathbf{B}_-(\mathbf{n})[\mathbf{w}] \cdot \mathbf{N}_\kappa \mathbf{B}_-(\mathbf{n})[\mathbf{v}] \, \mathrm{d}s$$

$$+\sum_{\kappa\in\mathcal{T}_h}\int_{\partial\kappa\cap\Gamma}\mathbf{B}_-(\boldsymbol{\mu})\mathbf{w}^+\cdot\mathbf{N}_\kappa\mathbf{B}_-(\boldsymbol{\mu})\mathbf{v}^+\,\mathrm{d}s\,. \tag{2.2}$$

Here, $\mathbf{M}_\kappa\in\mathbb{R}^{m\times m}_{\mathrm{symm}}$, $\mathbf{N}_\kappa\in\mathbb{R}^{m\times m}_{\mathrm{symm}}$, and $\mathbf{M}_\kappa$ and $\mathbf{N}_\kappa$ are bounded and positive definite, uniformly in $\kappa\in\mathcal{T}_h$, h and $\mathbf{p}$.

For $\mathbf{v}\in[H^1(\Omega,\mathcal{T}_h)]^m$, we consider the linear functional

$$\ell_{\mathrm{LS}}(\mathbf{v})=\sum_{\kappa\in\mathcal{T}_h}\frac{h_\kappa}{p_\kappa}\int_\kappa\mathbf{f}\cdot\mathbf{M}_\kappa\mathcal{L}\mathbf{v}\,\mathrm{d}x+\sum_{\kappa\in\mathcal{T}_h}\int_{\partial\kappa\cap\Gamma}\mathbf{B}_-(\mathbf{n})\,\mathbf{g}\cdot\mathbf{N}_\kappa\mathbf{B}_-(\mathbf{n})\mathbf{v}^+\,\mathrm{d}s\,. \tag{2.3}$$

The hp–LS-DGFEM for (2.1) is defined as follows: find $\mathbf{u}_{\mathrm{LS}}\in S^{\mathbf{p}}(\Omega,\mathcal{T}_h,\mathbf{F})$ such that

$$B_{\mathrm{LS}}(\mathbf{u}_{\mathrm{LS}},\mathbf{v})=\ell_{\mathrm{LS}}(\mathbf{v})\quad\forall\mathbf{v}\in S^{\mathbf{p}}(\Omega,\mathcal{T}_h,\mathbf{F})\,. \tag{2.4}$$

The existence of a unique solution to (2.4) is easy to verify: as

$$B_{\mathrm{LS}}(\mathbf{w},\mathbf{w})>0\qquad\forall\mathbf{w}\in S^{\mathbf{p}}(\Omega,\mathcal{T}_h,\mathbf{F})\setminus\{\mathbf{0}\}\,,$$

the uniqueness of solutions to (2.4) follows; further, since (2.4) is a linear problem over the finite–dimensional space $S^{\mathbf{p}}(\Omega,\mathcal{T}_h,\mathbf{F})$, the existence of a solution is the consequence of its uniqueness.

3 Error analysis

Now, we embark on the error analysis of (2.4). We shall suppose throughout that $\mathbf{u}$, the solution to our model problem (2.1), is sufficiently smooth in the sense that $\mathbf{u}\in[H^1(\Omega,\mathcal{T}_h)]^m$ and $\mathbf{B}_-(\mathbf{n})[\mathbf{u}]|_{\partial\kappa}=\mathbf{0}$ for any $\kappa\in\mathcal{T}_h$ (we note that a sufficient condition for this to hold is that $\mathbf{u}\in[H^1(\Omega)]^m$). Under this hypothesis, we have the following Galerkin orthogonality property:

$$B_{\mathrm{LS}}(\mathbf{u}-\mathbf{u}_{\mathrm{LS}},\mathbf{v})=0\qquad\forall\mathbf{v}\in S^{\mathbf{p}}(\Omega,\mathcal{T}_h,\mathbf{F})\,.$$

We define the norm $|||\cdot|||_{\mathrm{LS}}$ on $[H^1(\Omega,\mathcal{T}_h)]^m$ by $|||\,\mathbf{w}|||^2_{\mathrm{LS}}=B_{\mathrm{LS}}(\mathbf{w},\mathbf{w})$. Thus,

$$|||\,\mathbf{u}-\mathbf{u}_{\mathrm{LS}}|||^2_{\mathrm{LS}}=B_{\mathrm{LS}}(\mathbf{u}-\mathbf{u}_{\mathrm{LS}},\mathbf{u}-\mathbf{u}_{\mathrm{LS}})=B_{\mathrm{LS}}(\mathbf{u}-\mathbf{u}_{\mathrm{LS}},\mathbf{u}-\mathbf{v})$$

for all $\mathbf{v}\in S^{\mathbf{p}}(\Omega,\mathcal{T}_h,\mathbf{F})$. Hence, on applying the Cauchy–Schwarz inequality on the right–hand side,

$$|||\,\mathbf{u}-\mathbf{u}_{\mathrm{LS}}|||_{\mathrm{LS}}=\inf_{\mathbf{v}\in S^{\mathbf{p}}(\Omega,\mathcal{T}_h,\mathbf{F})}|||\,\mathbf{u}-\mathbf{v}|||_{\mathrm{LS}}\,. \tag{3.5}$$

In the sequel, for the sake of simplicity, we shall suppose that Ω has been partitioned into elements $\kappa\in\mathcal{T}_h$ each of which is a (bijective) affine image of the reference hypercube $\hat{\kappa}=(-1,1)^d$. We recall from [9] the following approximation result; see also the monograph of Schwab [18], Theorem 3.17 on p.76.

Lemma 3.1 Suppose that $\mathbf{u} \in [H^{k_\kappa+1}(\kappa)]^m$ for $\kappa \in \mathcal{T}_h$. Then, there exists $\Pi\mathbf{u} \in S^{\mathbf{p}}(\Omega, \mathcal{T}_h, \mathbf{F})$ such that, for $p_\kappa \geq 1$ and $0 \leq s_\kappa \leq \min(p_\kappa, k_\kappa)$, we have

$$\|\mathbf{u} - \Pi\mathbf{u}\|^2_{[L_2(\kappa)]^m} \leq C \left(\frac{h_\kappa}{2}\right)^{2s_\kappa+2} \frac{1}{p_\kappa(p_\kappa+1)} \Phi(p_\kappa, s_\kappa) |\mathbf{u}|^2_{[H^{s_\kappa+1}(\kappa)]^m}$$

and

$$|\,\mathbf{u} - \Pi\mathbf{u}|^2_{[H^1(\kappa)]^m} \leq C \left(\frac{h_\kappa}{2}\right)^{2s_\kappa} \Phi(p_\kappa, s_\kappa) |\mathbf{u}|^2_{[H^{s_\kappa+1}(\kappa)]^m}\,,$$

where

$$\Phi(p,s) = \frac{(p-s)!}{(p+s)!} + \frac{1}{p(p+1)} \frac{(p-s+1)!}{(p+s-1)!}\,, \qquad 0 \leq s \leq p\,,$$

and C is an absolute constant independent of h_κ, p_κ and $\mathbf{u}$.

Inserting these bounds into the multiplicative trace inequality

$$\|\,w\|^2_{L_2(\partial\kappa)} \leq C \left(h_\kappa^{-1}\|w\|^2_{L_2(\kappa)} + \|w\|_{L_2(\kappa)}|w|_{H^1(\kappa)}\right)\,, \qquad w \in H^1(\kappa)\,,$$

we deduce the following error estimate.

Corollary 3.2 Under the hypotheses of Lemma 3.1,

$$\|\mathbf{u} - \Pi\mathbf{u}\|^2_{[L_2(\partial\kappa)]^m} \leq C \left(\frac{h_\kappa}{2}\right)^{2s_\kappa+1} \Phi_1(p_\kappa, s_\kappa) |\mathbf{u}|^2_{[H^{s_\kappa+1}(\kappa)]^m}\,,$$

where

$$\Phi_1(p,s) = \frac{1}{\sqrt{p(p+1)}}\, \Phi(p,s)\,,$$

and C is an absolute constant independent of h_κ, p_κ and $\mathbf{u}$.

In order to complete the error analysis we need to quantify $|||\mathbf{u}-\Pi\mathbf{u}|||_{\mathrm{LS}}$. This is easily achieved by substituting the last three error bounds into the definition of the norm $|||\cdot|||_{\mathrm{LS}}$.

Corollary 3.3 Under the hypotheses of Lemma 3.1 we have that

$$|||\mathbf{u} - \Pi\mathbf{u}|||^2_{\mathrm{LS}} \leq C \sum_{\kappa\in\mathcal{T}_h} \left(\frac{h_\kappa}{2}\right)^{2s_\kappa+1} L_\kappa \Phi_1(p_\kappa, s_\kappa) |\mathbf{u}|^2_{[H^{s_\kappa+1}(\kappa)]^m}\,,$$

where

$$\begin{aligned} L_\kappa \;=\; & \|\mathbf{M}_\kappa\|_{[L_\infty(\kappa)]^{m\times m}} \left(\|\mathbf{B}\|^2_{[L_\infty(\kappa)]^{m\times m}} + \Big\|\mathbf{C} + \sum_{j=1}^d \frac{\partial \mathbf{B}_j}{\partial x_j}\Big\|^2_{[L_\infty(\kappa)]^{m\times m}} \right) \\ & + \|\mathbf{N}_\kappa\|_{[L_\infty(\partial\kappa)]^{m\times m}} \|\mathbf{B}_-(\mathbf{n})\|^2_{[L_\infty(\partial\kappa)]^{m\times m}}\,, \end{aligned} \qquad (3.6)$$

and C is an absolute constant independent of h_κ, p_κ and $\mathbf{u}$.

Our final bound on the discretization error is a trivial consequence of (3.5) and Corollary 3.3.

Theorem 3.4 Suppose that $\mathbf{u} \in [H^{k_\kappa+1}(\kappa)]^m$ for each $\kappa \in \mathcal{T}_h$. Then, there exists a positive constant C, independent of h_κ, p_κ and $\mathbf{u}$ such that, for $p_\kappa \geq 1$ and $0 \leq s_\kappa \leq \min(p_\kappa, k_\kappa)$, we have

$$|||\mathbf{u} - \mathbf{u}_{\mathrm{LS}}|||_{\mathrm{LS}}^2 \leq C \sum_{\kappa \in \mathcal{T}_h} \left(\frac{h_\kappa}{2}\right)^{2s_\kappa+1} L_\kappa \Phi_1(p_\kappa, s_\kappa) |\mathbf{u}|^2_{[H^{s_\kappa+1}(\kappa)]^m} \,,$$

where L_κ is defined by (3.6).

We conclude this section by an observation concerning the optimality of the last error bound.

Remark 3.5 A simple application of Stirling's formula shows that

$$\Phi_1(p, s) = C(s) p^{-(2s+1)}$$

for all $p \geq 1$. Hence, Theorem 3.4 gives

$$|||\mathbf{u} - \mathbf{u}_{\mathrm{LS}}|||_{\mathrm{LS}}^2 \leq C \sum_{\kappa \in \mathcal{T}_h} L_\kappa \left(\frac{h_\kappa}{p_\kappa}\right)^{2s_\kappa+1} |\mathbf{u}|^2_{[H^{s_\kappa+1}(\kappa)]^m}$$

with $p_\kappa \geq 1$ for all $\kappa \in \mathcal{T}_h$; this is optimal with respect to both h_κ and p_κ.

Now, suppose that $\mathbf{u}$ is *element-wise analytic* on $\mathcal{T}_h$ in the sense that for each $\kappa \in \mathcal{T}_h$ the function $\mathbf{u}|_\kappa$ has analytic extension to an open set, independent of h_κ, containing $\bar{\kappa}$. Then,

$$\exists d_\kappa > 0 \quad \exists C = C(\mathbf{u}) > 0 \quad \forall s \geq 0 \quad |\mathbf{u}|_{[H^s(\kappa)]^m} \leq C(\mathbf{u})(d_\kappa)^s \, s! \, |\mathrm{meas}(\kappa)|^{\frac{1}{2}} \,.$$

By means of Stirling's formula, after a rather straightforward but lengthy calculation, as in [9], we deduce from Theorem 3.4 the following result.

Theorem 3.6 Let $\Omega \subset \mathbb{R}^d$ be a bounded polyhedral domain, $\mathcal{T}_h = \{\kappa\}$ a shape–regular subdivision of Ω into d-parallelepipeds. Suppose that $\mathbf{u}$ is elementwise analytic on $\mathcal{T}_h$. Then, the solution $\mathbf{u}_{\mathrm{LS}} \in S^{\mathbf{p}}(\Omega, \mathcal{T}_h, \mathbf{F})$ of (2.4), with $p_\kappa \geq 1$ for $\kappa \in \mathcal{T}_h$, obeys the error bound

$$|||\mathbf{u} - \mathbf{u}_{\mathrm{LS}}|||_{\mathrm{LS}}^2 \leq C(\mathbf{u}) \sum_{\kappa \in \mathcal{T}_h} \left(\frac{h_\kappa}{2}\right)^{2s_\kappa+1} p_\kappa^2 e^{-2b_\kappa p_\kappa} |\, \mathrm{meas}(\kappa)| \,,$$

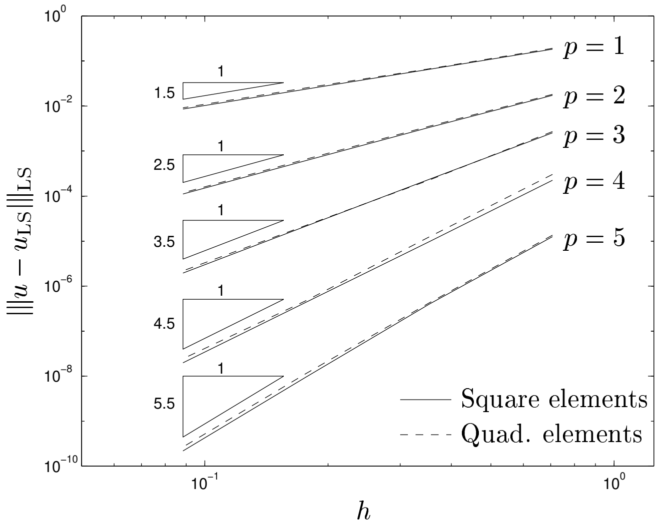

Figure 1: Example 1. Convergence of the hp–LS-DGFEM with h–refinement.

where $C(\mathbf{u})$ is a constant depending on $\mathbf{u}$, the dimension d, and the shape–regularity of $\mathcal{T}_h$; the real number b_κ is defined by

$$b_\kappa = \frac{1}{2}|\log F(\alpha_{\min}, d_\kappa)|\,,$$

where

$$\alpha_{\min} = (1+d^2)^{-1/2} \qquad \text{and} \qquad F(\alpha, d) = \frac{(1-\alpha)^{1-\alpha}}{(1+\alpha)^{1+\alpha}}\,(\alpha d)^{2\alpha}\,.$$

In the next section we shall verify the sharpness of our error bounds. We shall also demonstrate that even though LS-DGFEM exhibits the same asymptotic convergence rates as the classical DGFEM (cf. [9, 10]), it is not competitive with DGFEM as it suffers from excessive numerical dissipation.

4 Numerical experiments

In this section we present a series of numerical experiments both to verify the *a priori* error estimates derived in Section 3 and to investigate the practical performance of the hp–version LS-DGFEM.

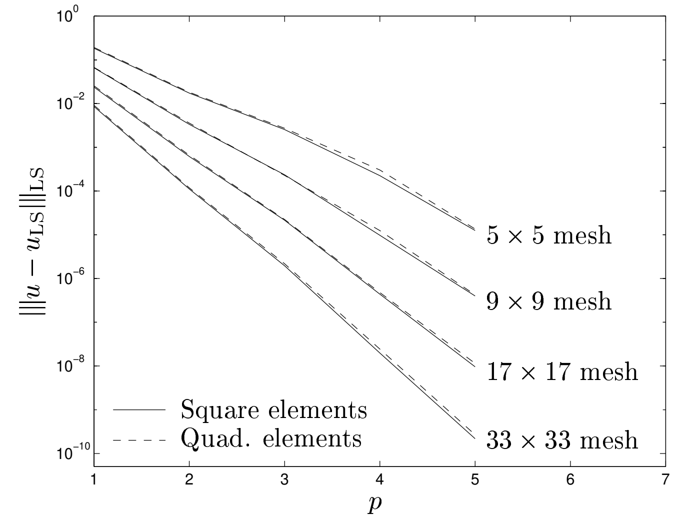

Figure 2: Example 1. Convergence of the hp–LS-DGFEM with p–refinement.

4.1 Example 1

In this first example we consider a scalar advection–reaction problem (i.e., $m = 1$) with smooth analytical solution. To this end, we let $\Omega = (-1,1)^2$, $\mathbf{B}(\mathbf{x}) = (b_1(x,y), b_2(x,y)) \equiv (8/10, 6/10)$, $\mathbf{C}(\mathbf{x}) = c(x,y) \equiv 1$, $\mathbf{g}(\mathbf{x}) = g(x,y) \equiv 1$ and $\mathbf{f}(\mathbf{x}) = f(x,y)$ is chosen so that the analytical solution to (2.1) is

$$\mathbf{u}(\mathbf{x}) \equiv u(x,y) = 1 + \sin(\pi(1+x)(1+y)^2/8)\,, \tag{4.7}$$

cf. [1, 9].

Here, we investigate the asymptotic behavior of the hp–version of the least–squares discontinuous Galerkin method on a sequence of successively finer square and quadrilateral meshes for different p. In each case the quadrilateral mesh is constructed from a uniform $N \times N$ square mesh by randomly perturbing each of the *interior* nodes by up to 10% of the local mesh–size, cf. [9].

In Figure 1 we present a comparison of the least–squares norm ($|||\cdot|||_{LS}$) of the error with the mesh function h for $1 \leq p \leq 5$. Here, we observe that $|||u - u_{LS}|||_{LS}$ converges to zero, for each fixed p, at the rate $\mathcal{O}(h^{p+1/2})$ as the mesh is refined, in agreement with Theorem 3.4. Finally, we investigate the convergence of the hp–LS-DGFEM with p–enrichment on a fixed mesh. Since the true solution (4.7) is a real analytic function, we expect

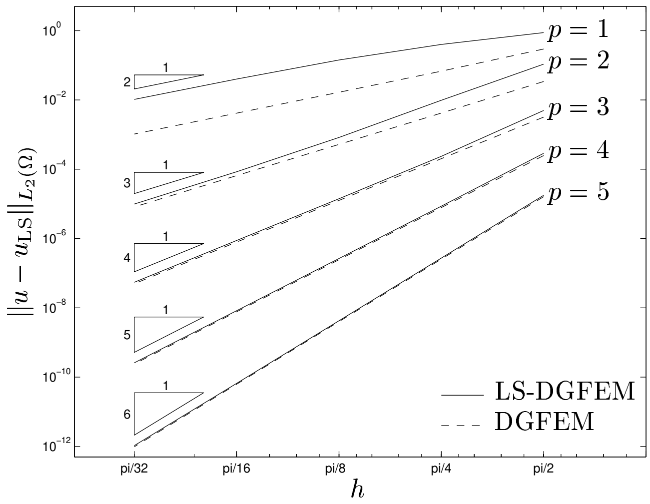

Figure 3: Example 2. Convergence of LS-DGFEM and DGFEM with h–refinement.

to see exponential rates of convergence as p increases. In Figure 2, we plot the least–squares norm of the error against p on four different square and quadrilateral meshes. In each case, we observe that on a linear–log scale, the convergence plots become straight lines as the spectral order p is increased, thereby indicating exponential convergence in p, cf. Theorem 3.6. Furthermore, we observe from Figures 1 & 2 that the h– and p– convergence of the hp–version LS-DGFEM is robust with respect to mesh distortion.

4.2 Example 2

Our second experiment compares the accuracy of LS-DGFEM with that of DGFEM for a one-dimensional model problem with smooth solution. We let $\Omega = (0, \pi)$ and select

$$\mathbf{B} \equiv \begin{pmatrix} 1 & 0 \\ 0 & -1 \end{pmatrix}, \ \mathbf{C} \equiv \begin{pmatrix} 0 & 1 \\ 1 & 0 \end{pmatrix}, \ \mathbf{f} \equiv \begin{pmatrix} 0 \\ 0 \end{pmatrix}, \ \mathbf{g}(0) = -\mathbf{g}(\pi) = \begin{pmatrix} 1 \\ 0 \end{pmatrix}.$$

The solution to this model problem is $\mathbf{u} = (\cos(x), \sin(x))^T$. Figure 3 indicates that both LS-DGFEM and DGFEM achieve optimal convergence rates in the L_2–norm for this system. However, while we observe that for $p \geq 3$ the errors of the two schemes are virtually identical, this is not so for $p \leq 2$; indeed, in the latter case DGFEM delivers more accurate results than LS-DGFEM on each of the uniform subdivisions of the interval $(0, \pi)$

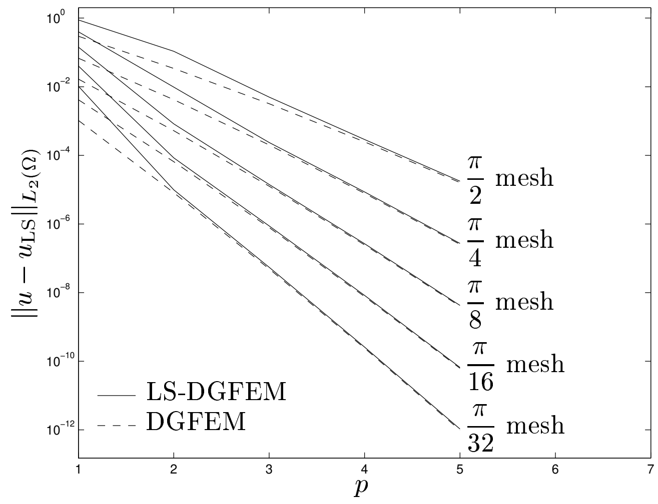

Figure 4: Example 2. Convergence of LS-DGFEM and DGFEM with p–refinement.

considered. This can also be seen in Figure 4 which shows the L_2–error against the polynomial degree.

In order to understand the observed behavior, let us consider a somewhat simpler scalar problem on $\Omega = (-1, 1)$, with $\mathcal{T} = \{\Omega\}$, $\mathbf{B} \equiv 1$ and $\mathbf{C} \equiv 0$. Here the LS-DGFEM approximation can be expressed in closed form in terms of Legendre polynomials as

$$\begin{aligned} u_{\mathrm{LS}}(x) &= \sum_{i=0}^{p-2} \frac{2i+1}{2} \left(\int_{-1}^{1} L_i(\xi) u(\xi) \, \mathrm{d}\xi \right) L_i(x) \\ &\quad + \sum_{i=p-1}^{p} \frac{1}{2} \left(\int_{-1}^{1} L_{i-1}(\xi) u'(\xi) \, \mathrm{d}\xi \right) L_i(x) \, . \end{aligned}$$

Similarly, for DGFEM we obtain

$$\begin{aligned} u_{\mathrm{DG}}(x) &= \sum_{i=0}^{p-1} \frac{2i+1}{2} \left(\int_{-1}^{1} L_i(\xi) u(\xi) \, \mathrm{d}\xi \right) L_i(x) \\ &\quad + \left(\sum_{j=p}^{\infty} \frac{2j+1}{2} \int_{-1}^{1} L_j(\xi) u(\xi) \, \mathrm{d}\xi \right) L_p(x) \, . \end{aligned}$$

To derive these identities we used integration by parts, the formula $L_n = (L'_{n+1} - L'_{n-1})/(2n+1)$, $n \geq 1$, and the orthogonality of Legendre poly-

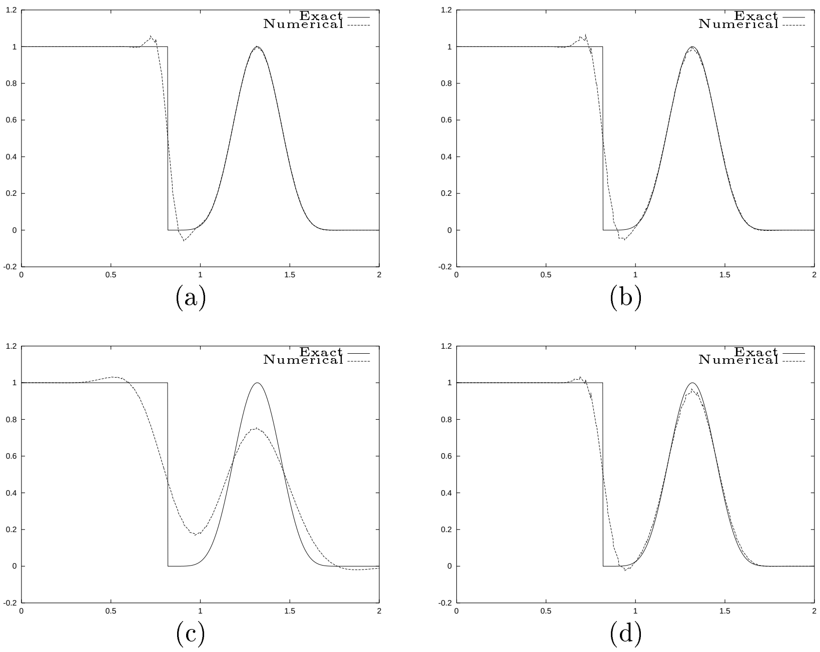

Figure 5: Example 3. Outflow profiles along $0 \leq x \leq 2$, $y = 1$, computed using DGFEMs on a 65×33 mesh with piecewise bilinear elements ($p = 1$): (a) Standard DGFEM; (b) Streamline–diffusion stabilized DGFEM; (c) LS-DGFEM; (d) Unsymmetric LS-DGFEM.

nomials in the inner product of $L_2(-1, 1)$. Comparing u_{LS} with u_{DG} we see that for $p \geq 3$ the first $p - 2$ terms in the expansions of u_{LS} and u_{DG} coincide; due to the fact that u is an entire analytic function on $\mathbb{R}$, the higher order Legendre modes decay very quickly and hence the difference between u_{LS} and u_{DG} is small for $p \geq 3$, particularly for large p.

4.3 Example 3

In this third experiment we assess the practical performance of the *hp*–LS-DGFEM for a scalar linear advection problem with discontinuous boundary data. We let $\Omega = (0, 2) \times (0, 1)$, $\mathbf{B}(\mathbf{x}) = (b_1(x, y), b_2(x, y)) \equiv (1 +$

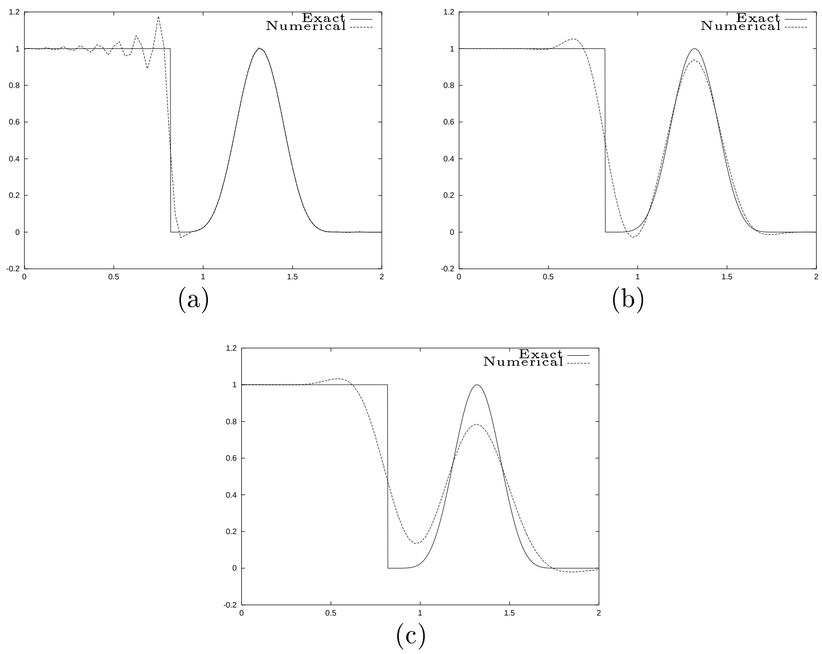

Figure 6: Example 3. Outflow profiles along $0 \leq x \leq 2$, $y = 1$, computed using continuous finite element methods on a 65×33 mesh with piecewise bilinear elements ($p = 1$): (a) Standard CGFEM; (b) Streamline–diffusion stabilized CGFEM; (c) Least–squares CGFEM.

$\sin(\pi y/2), 2)$, $\mathbf{C}(\mathbf{x}) = c(x, y) \equiv 0$, $\mathbf{f}(\mathbf{x}) = f(x, y) \equiv 0$ and

$$\mathbf{g}(\mathbf{x}) \equiv g(x, y) = \begin{cases} 1, & x = 0,\ 0 \leq y \leq 1\,, \\ \sin^6(\pi x), & 0 < x \leq 1,\ y = 0\,, \\ 0, & 1 \leq x \leq 2,\ y = 0\,. \end{cases}$$

In Figure 5, we compare the performance of the LS-DGFEM with the standard discontinuous Galerkin method (DGFEM), and the streamline–diffusion stabilized discontinuous Galerkin method (SD-DGFEM). In each case, we show the outflow profile along the horizontal edge $0 \leq x \leq 2$, $y = 1$ on a 65×33 uniform square mesh with discontinuous piecewise bilinear elements ($p = 1$). We observe that the performance of the DGFEM and the SD-DGFEM are very similar, cf. [9]; in each case the smooth hill is extremely well approximated, with some under–shoots and over–shoots present in the vicinity of the discontinuity in the analytical solution. In contrast, the LS-DGFEM is overly–diffusive leading to the excessive smearing of both the discontinuity and the smooth hill present in the analytical solution, cf. Figure 5(c) . We remark that the numerical dissipation inherent in the LS-DGFEM is due to the inclusion of the least–squares stabilization into the interelement jump terms rather than the presence of the least–squares stabilization in the element–integral terms. Indeed, in Figure 5(d) we show the solution generated by employing an unsymmetric least–squares discontinuous Galerkin finite element method where the element integral terms are identical to those in LS-DGFEM (cf. the first term in (2.2) and the first term in (2.3)) while the interelement jump terms and the boundary terms are identical to those arising in the standard DGFEM. Here, we observe that even though this unsymmetric least–squares method is more dissipative than both DGFEM and SD-DGFEM, the excessive smearing inherent in the LS-DGFEM has now been eradicated. Motivated by these observations, in the following section we consider the analysis of a general class of discontinuous Galerkin schemes including DGFEM and LS-DGFEM as well as possibly new ones.

However, before concluding this section, we compare the performance of the *hp*–LS-DGFEM with the standard, streamline–diffusion stabilized and the Galerkin least–squares finite element methods based on *continuous* piecewise polynomials. In Figure 6 we show the outflow profiles of each of the aforementioned schemes; here, we again observe that the LS-CGFEM excessively smears–out the solution, though the level of dissipation is slightly less than when the LS-DGFEM is employed.

5 A general family of DGFEMs

In this section, we embed LS-DGFEM into a one-parameter family of discontinuous Galerkin finite element methods, which also includes DGFEM. We begin by recalling the DGFEM approximation of (2.1). We adopt the following (standard) hypothesis: there exists a vector $\boldsymbol{\xi} \in \mathbb{R}^d$ such that

$$\frac{1}{2}\left(\mathbf{C}(\mathbf{x}) + \mathbf{C}^T(\mathbf{x})\right) + \frac{1}{2}\,(\nabla \cdot \mathbf{B})(\mathbf{x}) + \mathbf{B}(\mathbf{x}) \cdot \boldsymbol{\xi} \geq \gamma_0\,\mathbf{Id} \qquad \text{a.e. } \mathbf{x} \in \Omega\,, \quad (5.8)$$

where $\gamma_0 > 0$ is a constant. For simplicity of presentation, we shall assume throughout that (5.8) may be satisfied with $\boldsymbol{\xi} \equiv 0$; we then define the positive definite matrix $\mathbf{C}_0$ by

$$\mathbf{C}_0(\mathbf{x}) = \frac{1}{2}\left(\mathbf{C}(\mathbf{x}) + \mathbf{C}^T(\mathbf{x})\right) + \frac{1}{2}\,(\nabla \cdot \mathbf{B})(\mathbf{x}) \qquad \text{a.e. } \mathbf{x} \in \Omega\,. \qquad (5.9)$$

Further, we let $\gamma_1 = \max_{\mathbf{x} \in \bar{\Omega}} \|\mathbf{C}_0(\mathbf{x})\|_2$, where $\|\cdot\|_2$ denotes the matrix norm on $\mathbb{R}^{m\times m}$ subordinate to the Euclidean norm on $\mathbb{R}^m$. For $\mathbf{v}, \mathbf{w} \in$

$[H^1(\Omega,\mathcal{T}_h)]^m$ we consider the bilinear form

$$\begin{aligned} B_{\mathrm{DG}}(\mathbf{w},\mathbf{v}) &= \sum_{\kappa\in\mathcal{T}_h}\int_\kappa \mathbf{w}\cdot\mathcal{L}^*\mathbf{v}\,\mathrm{d}x + \sum_{\kappa\in\mathcal{T}_h}\int_{\partial\kappa\cap\Gamma}\mathbf{B}_+(\boldsymbol{\mu})\,\mathbf{w}^+\cdot\mathbf{v}^+\,\mathrm{d}s \\ &\quad + \sum_{\kappa\in\mathcal{T}_h}\int_{\partial\kappa\setminus\Gamma}(\mathbf{B}_+(\mathbf{n})\mathbf{w}^+ + \mathbf{B}_-(\mathbf{n})\mathbf{w}^-)\cdot\mathbf{v}^+\,\mathrm{d}s \qquad (5.10)\end{aligned}$$

and the linear functional

$$\ell_{\mathrm{DG}}(\mathbf{v}) = \sum_{\kappa\in\mathcal{T}_h}\int_\kappa \mathbf{f}\cdot\mathbf{v}\,\mathrm{d}x - \sum_{\kappa\in\mathcal{T}_h}\int_{\partial\kappa\cap\Gamma}\mathbf{B}_-(\boldsymbol{\mu})\,\mathbf{g}_{\mathrm{D}}\cdot\mathbf{v}^+\,\mathrm{d}s\,. \qquad (5.11)$$

The DGFEM approximation of (2.1) is defined as follows: find $\mathbf{u}_{\mathrm{DG}} \in S^{\mathbf{p}}(\Omega,\mathcal{T}_h,\mathbf{F})$ such that

$$B_{\mathrm{DG}}(\mathbf{u}_{\mathrm{DG}},\mathbf{v}) = \ell_{\mathrm{DG}}(\mathbf{v}) \quad \forall\mathbf{v}\in S^{\mathbf{p}}(\Omega,\mathcal{T}_h,\mathbf{F})\,. \qquad (5.12)$$

For a detailed stability and error analysis of this method in the case of a scalar multi-dimensional hyperbolic problem we refer to the articles [9] and [10]. For the present purposes it is sufficient to note that

$$\begin{aligned} B_{\mathrm{DG}}(\mathbf{v},\mathbf{v}) &= \sum_{\kappa\in\mathcal{T}_h}\int_\kappa \mathbf{C}_0\mathbf{v}\cdot\mathbf{v}\,\mathrm{d}x + \frac{1}{2}\sum_{\kappa\in\mathcal{T}_h}\int_{\partial\kappa\setminus\Gamma} -\mathbf{B}_-(\mathbf{n})[\mathbf{v}]\cdot[\mathbf{v}]\,\mathrm{d}s \\ &\quad + \frac{1}{2}\int_{\partial\kappa\cap\Gamma}(\mathbf{B}_+(\boldsymbol{\mu}) - \mathbf{B}_-(\boldsymbol{\mu}))\,\mathbf{v}\cdot\mathbf{v}\,\mathrm{d}s \equiv |||\mathbf{v}|||^2_{\mathrm{DG}}\,. \qquad (5.13)\end{aligned}$$

Now suppose that $t\in[0,1]$. Let us define the bilinear form

$$B_t(\mathbf{w},\mathbf{v}) = (1-t)\,B_{\mathrm{LS}}(\mathbf{w},\mathbf{v}) + t\,B_{\mathrm{DG}}(\mathbf{w},\mathbf{v})\,,$$

and the linear functional

$$\ell_t(\mathbf{v}) = (1-t)\,\ell_{\mathrm{LS}}(\mathbf{v}) + t\,\ell_{\mathrm{DG}}(\mathbf{v})\,.$$

We consider the following approximation of (2.1) which we shall henceforth refer to as tLS-DGFEM: find $\mathbf{u}_{hp}\in S^{\mathbf{p}}(\Omega,\mathcal{T}_h,\mathbf{F})$ such that

$$B_t(\mathbf{u}_{hp},\mathbf{v}) = \ell_t(\mathbf{v}) \qquad \forall\mathbf{v}\in S^{\mathbf{p}}(\Omega,\mathcal{T}_h,\mathbf{F})\,. \qquad (5.14)$$

Clearly,

$$B_t(\mathbf{v},\mathbf{v}) = (1-t)\,|||\mathbf{v}|||^2_{\mathrm{LS}} + t\,|||\mathbf{v}|||^2_{\mathrm{DG}} > 0 \;\; \forall\mathbf{v}\in S^{\mathbf{p}}(\Omega,\mathcal{T}_h,\mathbf{F})\setminus\{\mathbf{0}\}\,. \quad (5.15)$$

Consequently, (5.14) has a unique solution $\mathbf{u}_{hp}\in S^{\mathbf{p}}(\Omega,\mathcal{T}_h,\mathbf{F})$.

Next we turn our attention to the error analysis of tLS-DGFEM. As the case of $t=0$ has already been dealt with in Section 2, and hp–DGFEM, corresponding to $t=1$ has been shown to be hp–optimally convergent in [10], we shall confine our analysis to the case when $t \in (0,1)$.

First, we shall weaken the hypotheses of Section 3 on $\mathbf{M}_\kappa$ and $\mathbf{N}_\kappa$ by supposing instead that $\mathbf{M}_\kappa \in \mathbb{R}^{m\times m}_{\mathrm{symm}}$ and $\mathbf{N}_\kappa \in \mathbb{R}^{m\times m}_{\mathrm{symm}}$ are bounded, uniformly in $\kappa \in \mathcal{T}_h$, h and $\mathbf{p}$, and there exists a constant $\mu_0 \in (0,t)$, independent of h and $\mathbf{p}$ such that, for all κ in $\mathcal{T}_h$,

$$\left\{\begin{aligned} \mathbf{M}_\kappa \geq \mu_0 \mathbf{Id} \quad & \text{and} \\ (-\mathbf{B}_-)(\mathbf{n})\,\{2(1-t)\,\mathbf{N}_\kappa(-\mathbf{B}_-)(\mathbf{n}) + (t-\mu_0)\,\mathbf{Id}\} \geq \mathbf{0} \quad & \text{on } \partial\kappa\,. \end{aligned}\right. \tag{5.16}$$

For example, the second condition in (5.16) is satisfied with $\mathbf{N}_\kappa \equiv 0$ for all $\kappa \in \mathcal{T}_h$; indeed, $\mathbf{N}_\kappa$ need not even be positive semidefinite; it suffices that

$$(-\mathbf{B}_-)(\mathbf{n})\mathbf{N}_\kappa(-\mathbf{B}_-)(\mathbf{n}) \geq -\tau\,(-\mathbf{B}_-)(\mathbf{n})\,, \quad \text{where} \quad \tau = \frac{t-\mu_0}{2(1-t)}\,. \tag{5.17}$$

This means that, locally, the level of numerical dissipation in tLS-DGFEM can be reduced or increased beyond that of the basic DGFEM, which is a helpful computational device.

We begin the error analysis of tLS-DGFEM by observing that if $\mathbf{u} \in [H^1(\Omega,\mathcal{T}_h)]^m$ and $\mathbf{B}_-(\mathbf{n})[\mathbf{u}] = \mathbf{0}$ for all $\kappa \in \mathcal{T}_h$, then

$$B_t(\mathbf{u}-\mathbf{u}_{hp},\mathbf{v}) = 0 \qquad \forall \mathbf{v} \in S^{\mathbf{p}}(\Omega,\mathcal{T}_h,\mathbf{F})\,. \tag{5.18}$$

On decomposing $\mathbf{u}-\mathbf{u}_{hp} = \boldsymbol{\xi}+\boldsymbol{\eta}$ where $\boldsymbol{\xi} = \Pi\mathbf{u}-\mathbf{u}_{hp}$ and $\boldsymbol{\eta} = \mathbf{u}-\Pi\mathbf{u}$, with $\Pi\mathbf{u}$ defined as in Section 3, we conclude from (5.18) that

$$\begin{aligned} B_t(\boldsymbol{\xi},\boldsymbol{\xi}) = -B_t(\boldsymbol{\eta},\boldsymbol{\xi}) \quad &= \quad -(1-t)\,B_{\mathrm{LS}}(\boldsymbol{\eta},\boldsymbol{\xi}) - tB_{\mathrm{DG}}(\boldsymbol{\eta},\boldsymbol{\xi}) \\ &\equiv \quad \mathrm{T}_1 + \mathrm{T}_2\,. \end{aligned} \tag{5.19}$$

We begin by estimating the left–hand side of (5.19) from below. We deduce from (5.13) and the definition of $B_{\mathrm{LS}}(\cdot,\cdot)$ that

$$\begin{aligned} B_t(\boldsymbol{\xi},\boldsymbol{\xi}) \quad = \quad & \sum_{\kappa\in\mathcal{T}_h}\left(t\int_\kappa \boldsymbol{\xi}\cdot\mathbf{C}_0\boldsymbol{\xi}\,\mathrm{d}x + (1-t)\int_\kappa \frac{h_\kappa}{p_\kappa}\mathcal{L}\boldsymbol{\xi}\cdot\mathbf{M}_\kappa\mathcal{L}\boldsymbol{\xi}\,\mathrm{d}x\right) \\ & +\frac{1}{2}\sum_{\kappa\in\mathcal{T}_h}\int_{\partial\kappa\setminus\Gamma}(-\mathbf{B}_-(\mathbf{n}))[\boldsymbol{\xi}]\cdot\{\,t\,\mathbf{Id}+2(1-t)\,\mathbf{N}_\kappa(-\mathbf{B}_-(\mathbf{n}))\}\,[\boldsymbol{\xi}]\,\mathrm{d}s \\ & +\frac{1}{2}\sum_{\kappa\in\mathcal{T}_h}\int_{\partial\kappa\cap\Gamma}(-\mathbf{B}_-(\boldsymbol{\mu}))\boldsymbol{\xi}^+\cdot\{\,t\,\mathbf{Id}+2(1-t)\,\mathbf{N}_\kappa(-\mathbf{B}_-(\boldsymbol{\mu}))\}\,\boldsymbol{\xi}^+\,\mathrm{d}s \\ & +\frac{t}{2}\sum_{\kappa\in\mathcal{T}_h}\int_{\partial\kappa\cap\Gamma}\mathbf{B}_+(\boldsymbol{\mu})\boldsymbol{\xi}^+\cdot\boldsymbol{\xi}^+\,\mathrm{d}s\,. \end{aligned}$$

Hence,

$$
\begin{aligned}
&B_t(\boldsymbol{\xi},\boldsymbol{\xi}) \geq t\gamma_0 \sum_{\kappa\in\mathcal{T}_h} \|\boldsymbol{\xi}\|^2_{L_2(\kappa)} + (1-t)\mu_0 \sum_{\kappa\in\mathcal{T}_h} \frac{h_\kappa}{p_\kappa}\|\mathcal{L}\boldsymbol{\xi}\|^2_{L_2(\kappa)} \\
&+\frac{1}{2}\mu_0 \sum_{\kappa\in\mathcal{T}_h} \|(-\mathbf{B}_-(\mathbf{n}))^{\frac{1}{2}}\,[\boldsymbol{\xi}]\|^2_{L_2(\partial\kappa\setminus\Gamma)} + \frac{1}{2}\mu_0 \sum_{\kappa\in\mathcal{T}_h} \|(-\mathbf{B}_-(\boldsymbol{\mu}))^{\frac{1}{2}}\,\boldsymbol{\xi}^+\|^2_{L_2(\partial\kappa\cap\Gamma)} \\
&+\frac{1}{2}t \sum_{\kappa\in\mathcal{T}_h} \|(\mathbf{B}_+(\boldsymbol{\mu}))^{\frac{1}{2}}\,\boldsymbol{\xi}^+\|^2_{L_2(\partial\kappa\cap\Gamma)}\,, \qquad (5.20)
\end{aligned}
$$

with $0<\mu_0<t<1$ and $\gamma_0>0$.

Next, we bound T_1 from above. Recall that $\mathbf{M}_\kappa$ and $\mathbf{N}_\kappa$ have been assumed uniformly bounded, independent of h_κ and p_κ; therefore, there exists a constant $\mu_1>0$, independent of h_κ and p_κ such that

$$
\mathbf{M}_\kappa \leq \mu_1\mathbf{Id} \quad\text{and}\quad |\mathbf{N}_\kappa| \leq \mu_1\mathbf{Id} \qquad \text{for all } \kappa\in\mathcal{T}_h\,.
$$

Further, as $\mathbf{B}_i \in [W^1_\infty(\Omega)]^{m\times m}_{\mathrm{symm}}$ for $i=1,\dots,m$, there exists a positive constant β_1 such that, with $\mathbf{n}=\mathbf{n}_\kappa$,

$$
\max\left(\|(-\mathbf{B})_-(\mathbf{n})(\mathbf{x})\|_2\,,\, \|\mathbf{B}_+(\mathbf{n})(\mathbf{x})\|_2\right) \leq \beta_1 \quad \forall\,\kappa\in\mathcal{T}_h \text{ and all } \mathbf{x}\in\partial\kappa\setminus\Gamma
$$

and, with $\boldsymbol{\mu}(\mathbf{x})=\boldsymbol{\mu}_\kappa(\mathbf{x})$ for $\mathbf{x}\in\partial\kappa\cap\Gamma$,

$$
\max\left(\|(-\mathbf{B})_-(\boldsymbol{\mu})(\mathbf{x})\|_2\,,\, \|\mathbf{B}_+(\boldsymbol{\mu})(\mathbf{x})\|_2\right) \leq \beta_1 \quad \forall\,\kappa\in\mathcal{T}_h \text{ and all } \mathbf{x}\in\partial\kappa\cap\Gamma\,,
$$

where, again, $\|\cdot\|_2$ denotes the matrix norm on $\mathbb{R}^{m\times m}$ subordinate to the Euclidean norm on $\mathbb{R}^m$. Thus,

$$
\begin{aligned}
\mathrm{T}_1 \quad\leq\quad & (1-t)\mu_1 \left(\sum_{\kappa\in\mathcal{T}_h} \frac{h_\kappa}{p_\kappa}\|\mathcal{L}\boldsymbol{\eta}\|^2_{L_2(\kappa)}\right)^{\frac{1}{2}} \left(\sum_{\kappa\in\mathcal{T}_h} \frac{h_\kappa}{p_\kappa}\|\mathcal{L}\boldsymbol{\xi}\|^2_{L_2(\kappa)}\right)^{\frac{1}{2}} \\
&+(1-t)\mu_1\beta_1 \left(\sum_{\kappa\in\mathcal{T}_h} \|(-\mathbf{B}_-(\mathbf{n}))^{\frac{1}{2}}[\boldsymbol{\eta}]\|^2_{L_2(\partial\kappa\setminus\Gamma)}\right)^{\frac{1}{2}} \\
&\quad\times\left(\sum_{\kappa\in\mathcal{T}_h} \|(-\mathbf{B}_-(\mathbf{n}))^{\frac{1}{2}}[\boldsymbol{\xi}]\|^2_{L_2(\partial\kappa\setminus\Gamma)}\right)^{\frac{1}{2}} \\
&+(1-t)\mu_1\beta_1 \left(\sum_{\kappa\in\mathcal{T}_h} \|(-\mathbf{B}_-(\boldsymbol{\mu}))^{\frac{1}{2}}\boldsymbol{\eta}^+\|^2_{L_2(\partial\kappa\cap\Gamma)}\right)^{\frac{1}{2}} \\
&\quad\times\left(\sum_{\kappa\in\mathcal{T}_h} \|(-\mathbf{B}_-(\boldsymbol{\mu}))^{\frac{1}{2}}\boldsymbol{\xi}^+\|^2_{L_2(\partial\kappa\cap\Gamma)}\right)^{\frac{1}{2}}. \qquad (5.21)
\end{aligned}
$$

Next we bound T_2 from above. To do so, we begin by noting that

$$\sum_{\kappa\in\mathcal{T}_h}\int_{\partial\kappa\setminus\Gamma}\mathbf{B}_+(\mathbf{n})\boldsymbol{\eta}^+\cdot\boldsymbol{\xi}^+\,\mathrm{d}s=-\sum_{\kappa\in\mathcal{T}_h}\int_{\partial\kappa\setminus\Gamma}\mathbf{B}_-(\mathbf{n})\boldsymbol{\eta}^-\cdot\boldsymbol{\xi}^-\,\mathrm{d}s\,,$$

and therefore,

$$\begin{aligned}&\left|\sum_{\kappa\in\mathcal{T}_h}\int_{\partial\kappa\setminus\Gamma}\left(\mathbf{B}_+(\mathbf{n})\boldsymbol{\eta}^++\mathbf{B}_-(\mathbf{n})\boldsymbol{\eta}^-\right)\boldsymbol{\xi}^+\,\mathrm{d}s\right|\\ &\leq\left(\sum_{\kappa\in\mathcal{T}_h}\|(-\mathbf{B}_-(\mathbf{n}))^{\frac12}\boldsymbol{\eta}^-\|^2_{L_2(\partial\kappa\setminus\Gamma)}\right)^{\frac12}\left(\sum_{\kappa\in\mathcal{T}_h}\|(-\mathbf{B}_-(\mathbf{n}))^{\frac12}[\boldsymbol{\xi}]\|^2_{L_2(\partial\kappa\setminus\Gamma)}\right)^{\frac12}.\end{aligned}$$

Hence, noting that $\mathcal{L}^*\boldsymbol{\xi}=-\mathcal{L}\boldsymbol{\xi}+2\mathbf{C}_0\boldsymbol{\xi}$, we deduce that

$$\begin{aligned}\mathrm{T}_2\leq{}&t\left(\sum_{\kappa\in\mathcal{T}_h}\frac{p_\kappa}{h_\kappa}\|\boldsymbol{\eta}\|^2_{L_2(\kappa)}\right)^{\frac12}\left(\sum_{\kappa\in\mathcal{T}_h}\frac{h_\kappa}{p_\kappa}\|\mathcal{L}\boldsymbol{\xi}\|^2_{L_2(\kappa)}\right)^{\frac12}\\ &+2t\gamma_1\left(\sum_{\kappa\in\mathcal{T}_h}\|\boldsymbol{\eta}\|^2_{L_2(\kappa)}\right)^{\frac12}\left(\sum_{\kappa\in\mathcal{T}_h}\|\boldsymbol{\xi}\|^2_{L_2(\kappa)}\right)^{\frac12}\qquad(5.22)\\ &+t\left(\sum_{\kappa\in\mathcal{T}_h}\|(-\mathbf{B}_-(\mathbf{n}))^{\frac12}\,\boldsymbol{\eta}^-\|^2_{L_2(\partial\kappa\setminus\Gamma)}\right)^{\frac12}\left(\sum_{\kappa\in\mathcal{T}_h}\|(-\mathbf{B}_-(\mathbf{n}))^{\frac12}\,[\boldsymbol{\xi}]\|^2_{L_2(\partial\kappa\setminus\Gamma)}\right)^{\frac12}\\ &+t\left(\sum_{\kappa\in\mathcal{T}_h}\|(\mathbf{B}_+(\boldsymbol{\mu}))^{\frac12}\,\boldsymbol{\eta}^+\|^2_{L_2(\partial\kappa\cap\Gamma)}\right)^{\frac12}\left(\sum_{\kappa\in\mathcal{T}_h}\|(\mathbf{B}_+(\boldsymbol{\mu}))^{\frac12}\,\boldsymbol{\xi}^+\|^2_{L_2(\partial\kappa\cap\Gamma)}\right)^{\frac12}.\end{aligned}$$

Upon inserting the upper bounds (5.21) and (5.22) on T_1 and T_2, respectively, and the lower bound (5.20) on $B_t(\boldsymbol{\xi},\boldsymbol{\xi})$ into (5.19), we find that

$$\begin{aligned}|||\boldsymbol{\xi}|||_t^2\equiv{}&\sum_{\kappa\in\mathcal{T}_h}\|\boldsymbol{\xi}\|^2_{L_2(\kappa)}+\sum_{\kappa\in\mathcal{T}_h}\frac{h_\kappa}{p_\kappa}\|\mathcal{L}\boldsymbol{\xi}\|^2_{L_2(\kappa)}+\sum_{\kappa\in\mathcal{T}_h}\|(-\mathbf{B}_-(\mathbf{n}))^{\frac12}\,[\boldsymbol{\xi}]\|^2_{L_2(\partial\kappa\setminus\Gamma)}\\ &+\sum_{\kappa\in\mathcal{T}_h}\|(-\mathbf{B}_-(\boldsymbol{\mu}))^{\frac12}\,\boldsymbol{\xi}^+\|^2_{L_2(\partial\kappa\cap\Gamma)}+\sum_{\kappa\in\mathcal{T}_h}\|(\mathbf{B}_+(\boldsymbol{\mu}))^{\frac12}\,\boldsymbol{\xi}^+\|^2_{L_2(\partial\kappa\cap\Gamma)}\\ \leq{}&\tau_1|||\boldsymbol{\eta}|||_t^*\,|||\boldsymbol{\xi}|||_t\,,\qquad(5.23)\end{aligned}$$

where $\tau_1=\tau_1(t,\gamma_0,\gamma_1,\mu_0,\mu_1,\beta_1)$ is a positive constant, independent of the discretization parameters, and

$$|||\boldsymbol{\eta}|||_t^*\;=\;\left(\sum_{\kappa\in\mathcal{T}_h}\left\{\frac{p_\kappa}{h_\kappa}\|\boldsymbol{\eta}\|^2_{L_2(\kappa)}+\frac{h_\kappa}{p_\kappa}\|\mathcal{L}\boldsymbol{\eta}\|^2_{L_2(\kappa)}+\|(-\mathbf{B}_-(\mathbf{n}))^{\frac12}[\boldsymbol{\eta}]\|^2_{L_2(\partial\kappa\setminus\Gamma)}\right.\right.$$

$$+\ \|(-\mathbf{B}_-(\mathbf{n}))^{\frac{1}{2}}\boldsymbol{\eta}^-\|^2_{L_2(\partial\kappa\setminus\Gamma)} + \|(-\mathbf{B}_-(\boldsymbol{\mu}))^{\frac{1}{2}}\boldsymbol{\eta}^+\|^2_{L_2(\partial\kappa\cap\Gamma)}$$
$$+\|(\mathbf{B}_+(\boldsymbol{\mu}))^{\frac{1}{2}}\boldsymbol{\eta}^+\|^2_{L_2(\partial\kappa\cap\Gamma)}\Big\}\Big)^{\frac{1}{2}} .$$

We thus conclude from (5.23) that

$$|||\mathbf{u}-\mathbf{u}_{hp}|||_t \le |||\boldsymbol{\xi}|||_t + |||\boldsymbol{\eta}|||_t \le \tau_1|||\boldsymbol{\eta}|||_t^* + |||\boldsymbol{\eta}|||_t ,$$

so to complete the error analysis we now only need to bound $|||\boldsymbol{\eta}|||_t^*$ and $|||\boldsymbol{\eta}|||_t$ in exactly the same manner as in Section 3. Thus we arrive at the following result.

Theorem 5.1 Suppose that (5.16) holds and that $\mathbf{u} \in [H^{k_\kappa+1}(\kappa)]^m$ for each $\kappa \in \mathcal{T}_h$. Then, for each $t \in (0,1)$ there exists a positive constant C, independent of h_κ, p_κ and $\mathbf{u}$, such that, for $p_\kappa \ge 1$ and $0 \le s_\kappa \le \min(p_\kappa, k_\kappa)$, we have

$$|||\mathbf{u}-\mathbf{u}_{hp}|||_t^2 \le C \sum_{\kappa\in\mathcal{T}_h} \left(\frac{h_\kappa}{2}\right)^{2s_\kappa+1} \Phi_1(p_\kappa, s_\kappa)|\mathbf{u}|^2_{[H^{s_\kappa+1}(\kappa)]^m} .$$

Remark 5.2 A simple application of Stirling's formula shows that

$$\Phi_1(p,s) = C(s)p^{-(2s+1)}$$

for all $p \ge 1$. Hence Theorem 5.1 gives

$$|||\mathbf{u}-\mathbf{u}_{hp}|||_t^2 \le C \sum_{\kappa\in\mathcal{T}_h} \left(\frac{h_\kappa}{p_\kappa}\right)^{2s_\kappa+1} |\mathbf{u}|^2_{[H^{s_\kappa+1}(\kappa)]^m}$$

with $p_\kappa \ge 1$, $0 \le s_\kappa \le \min(p_\kappa, k_\kappa)$, for all $\kappa \in \mathcal{T}_h$, where C is a positive constant independent of h_κ, p_κ and $\mathbf{u}$. This bound is optimal with respect to both h_κ and p_κ.

Now, suppose that $\mathbf{u}$ is *element-wise analytic* on $\mathcal{T}_h$ in the sense that for each $\kappa \in \mathcal{T}_h$ the function $\mathbf{u}|_\kappa$ has analytic extension to an open set, independent of h_κ, containing $\bar{\kappa}$. Then, analogously as in Section 3, we deduce from Theorem 5.1 the following result.

Theorem 5.3 Suppose that (5.16) holds and let $\Omega \subset \mathbb{R}^d$ be a bounded polyhedral domain, $\mathcal{T}_h = \{\kappa\}$ a shape–regular subdivision of Ω into d-parallelepipeds. Assume that $\mathbf{u}$ is elementwise analytic on $\mathcal{T}_h$. Then, for any $t \in (0,1)$, the solution $\mathbf{u}_{hp} \in S^{\mathbf{p}}(\Omega, \mathcal{T}_h, \mathbf{F})$ of (5.14), with $p_\kappa \ge 1$ for $\kappa \in \mathcal{T}_h$, obeys the error bound

$$|||\mathbf{u}-\mathbf{u}_{hp}|||_t^2 \le C(\mathbf{u}) \sum_{\kappa\in\mathcal{T}_h} \left(\frac{h_\kappa}{2}\right)^{2s_\kappa+1} p_\kappa^2 e^{-2b_\kappa p_\kappa} |\,\mathrm{meas}(\kappa)| ,$$

where $C(\mathbf{u})$ is a constant depending on $\mathbf{u}$, the dimension d, and the shape–regularity of $\mathcal{T}_h$; the real number b_κ is defined by $b_\kappa = |\log F(\alpha_{\min}, d_\kappa)|/2$, where

$$\alpha_{\min} = (1+d^2)^{-1/2} \qquad \text{and} \qquad F(\alpha, d) = \frac{(1-\alpha)^{1-\alpha}}{(1+\alpha)^{1+\alpha}}\,(\alpha d)^{2\alpha}\,.$$

6 Numerical experiments

In this section we shall explore the implementation of tLS–DGFEM and conduct numerical experiments to verify the sharpness of our analytical results.

6.1 Example 4

We consider the one–dimensional wave equation

$$\frac{\partial^2 \phi}{\partial t^2} - c^2 \frac{\partial^2 \phi}{\partial x^2} = 0. \tag{6.24}$$

We note that by defining $x_1 \equiv x$ and $x_2 \equiv t$, the second–order partial differential equation (6.24) can be rewritten as the symmetric first–order system

$$\begin{bmatrix} 0 & -c \\ -c & 0 \end{bmatrix} \begin{bmatrix} u_1 \\ u_2 \end{bmatrix}_{x_1} + \begin{bmatrix} 1 & 0 \\ 0 & 1 \end{bmatrix} \begin{bmatrix} u_1 \\ u_2 \end{bmatrix}_{x_2} = \begin{bmatrix} 0 \\ 0 \end{bmatrix}, \tag{6.25}$$

where $u_1 = \partial\phi/\partial x_2$ and $u_2 = c\partial\phi/\partial x_1$. Here we let $\Omega = (0,1)\times(0,1/2)$ and $c = 1/2$, with

$$u_1(x_1, 0) = 0 \qquad \text{and} \qquad u_2(x_1, 0) = c\, e^{-100(x_1 - 1/2)^2},$$

for $0 \le x_1 \le 1$; this is a variant of the test problem considered in [8].

In Figures 7 and 8 we compare the performance of the tLS-DGFEM with $t = 0$ (LS-DGFEM), $t = 1/2$ and $t = 1$ (DGFEM), using both h– and p–refinement, respectively, on uniform square meshes. For consistency, in each case the error is measured in terms of the $L_2(\Omega)$ norm. Here, we observe that the error in the DGFEM is always smaller than for the tLS-DGFEM with $t = 1/2$; though the error for this latter scheme is always smaller than for the LS-DGFEM. However, if we measure the error with respect to the $L_\infty(\Omega)$ norm, then we see that the tLS-DGFEM with $t = 1/2$ now has clear advantages over both the DGFEM and the LS-DGFEM. Indeed, from Figures 9 and 10, we see that for $p > 1$, the tLS-DGFEM with $t = 1/2$ now outperforms both DGFEM and LS-DGFEM on some

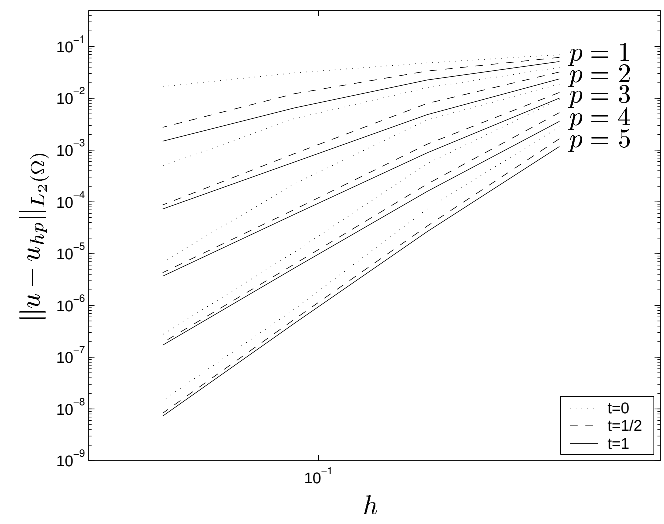

Figure 7: Example 4. Convergence of the tLS-DGFEM with h–refinement.

of the meshes employed; this is particularly noticeable on coarser grids. Thereby, we see that the dissipation present in the tLS-DGFEM, with $t = 1/2$, is large enough to provide additional stabilisation for higher p, cf. [9], yet small enough to ensure that the error is not adversely affected by the excessive dissipation present in the LS-DGFEM, cf. Section 4.3. Of course, the level of dissipation added into the standard DGFEM by combining it with the LS-DGFEM can be controlled by not only varying t, but also by allowing $\mathbf{M}_\kappa$ and $\mathbf{N}_\kappa$, cf. (2.2), to vary over each element κ in the mesh $\mathcal{T}_h$. Indeed, for a fixed t, $\mathbf{M}_\kappa$ and $\mathbf{N}_\kappa$ could be selected based on the size of the finite element residual to ensure the necessary 'tune-up' of the numerical dissipation in the vicinity of sharp features in the analytical solution $\mathbf{u}$; this work is part of our current research programme and will be presented elsewhere. In the present experiments we simply chose $\mathbf{M}_\kappa = \mathbf{N}_\kappa = \mathbf{Id}$ for all $\kappa \in \mathcal{T}_h$.

Acknowledgments

Paul Houston acknowledges the financial support of the EPSRC (Grant GR/N24230). Max Jensen thanks the DAAD ("Doktorandenstipendium im Rahmen des gemeinsamen Hochschulprogramms III von Bund und Ländern"), the Gottlieb Daimler- und Karl Benz-Stiftung and the Flughafen Frankfurt Main Stiftung for their sponsorship.

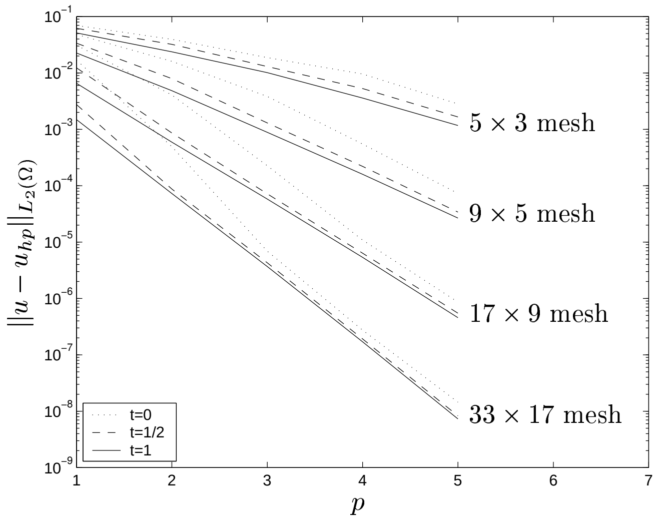

Figure 8: Example 4. Convergence of the tLS-DGFEM with p–refinement.

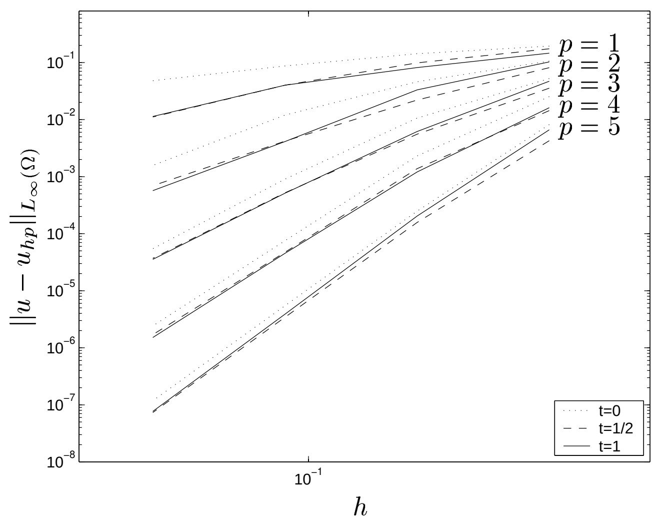

Figure 9: Example 4. Convergence of the tLS-DGFEM with h–refinement.

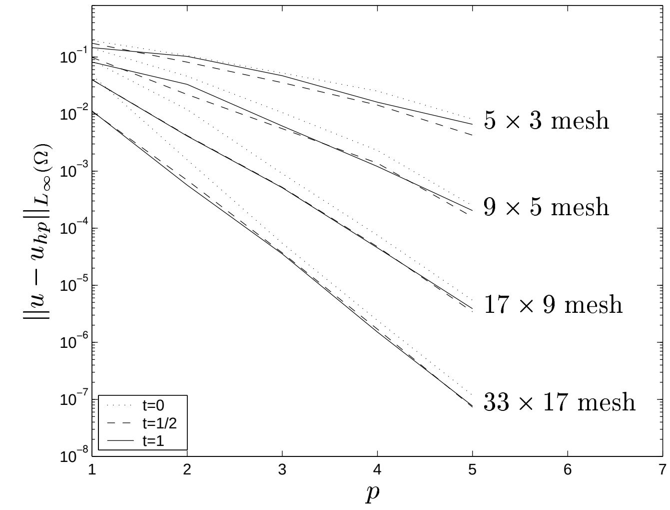

Figure 10: Example 4. Convergence of the tLS-DGFEM with p–refinement.

References

[1] K.S. Bey and J.T. Oden, *hp–Version discontinuous Galerkin methods for hyperbolic conservation laws,* Comput. Methods Appl. Mech. Engrg., 133 (1996), pp. 259–286.

[2] P.B. Bochev and M.D. Gunzburger, *Finite element methods of least–squares type,* SIAM Review, 40 (1998), pp. 789–893.

[3] B. Cockburn, S. Hou and C.-W. Shu, *TVB Runge–Kutta local projection discontinuous Galerkin finite elements for hyperbolic conservation laws,* Math. Comp., 54 (1990), pp. 545–581.

[4] B. Cockburn and C.-W. Shu, *TVB Runge–Kutta local projection discontinuous Galerkin finite element method for scalar conservation laws II: General framework,* Math. Comp., 52 (1989), pp. 411–435.

[5] B. Cockburn and C.-W. Shu, *The Runge–Kutta local projection P^1–discontinuous Galerkin method for scalar conservation laws,* Modél. Math. Anal. Numér., 25 (1991), pp. 337–361.

[6] B. Cockburn and C.-W. Shu, *The local discontinuous Galerkin method for time–dependent reaction–diffusion systems,* SIAM J. Numer. Anal., 35 (1998), pp. 2440–2463.

[7] B. Cockburn and C.-W. Shu, *The Runge–Kutta discontinuous Galerkin method for conservation laws: Multidimensional systems,* J. Comput. Phys., 141 (1998), pp. 199–244.

[8] P. Houston, J. Mackenzie, E. Süli, and G. Warnecke, *A posteriori error analysis for numerical approximations of Friedrichs systems,* Numer. Math. 82(3):433–470, 1999.

[9] P. Houston, Ch. Schwab and E. Süli, *Stabilized hp–finite element methods for first–order hyperbolic problems,* SIAM J. Numer. Anal., 37 (2000), pp. 1618–1643.

[10] P. Houston, Ch. Schwab and E. Süli, *Discontinuous hp–Finite Element Methods for Advection–Diffusion–Reaction Problems,* SIAM J. Numer. Anal. (Accepted for publication). Available from the URL:
`http://web.comlab.ox.ac.uk/oucl/publications/natr/na-00-15.html`

[11] P. Houston and E. Süli, *Stabilized hp–finite element approximation of partial differential equations with non-negative characteristic form,* Computing, 66(2001), pp. 99–119.

[12] T.J.R. Hughes and A.A. Brooks, *A multidimensional upwind scheme with no crosswind diffusion.* Finite element methods for convection dominated flows (Papers, Winter Ann. Meeting Amer. Soc. Mech. Engrs., New York, 1979), pp. 19–35, AMD, 34, Amer. Soc. Mech. Engrs. (ASME), New York, 1979.

[13] C. Johnson, U. Nävert and J. Pitkäranta, *Finite element methods for linear hyperbolic problems,* Comp. Meth. Appl. Mech. Engrg., 45 (1984), pp. 285–312.

[14] C. Johnson and J. Pitkäranta, *An analysis of the discontinuous Galerkin method for a scalar hyperbolic equation,* Math. Comp., 46 (1986), pp. 1–26.

[15] P. Lesaint and P.A. Raviart, *On a finite element method for solving the neutron transport equation,* in Mathematical aspects of Finite Elements in Partial Differential equations, C.A. deBoor, ed., Academic Press, New York, 1974, pp. 89–123.

[16] G. Richter, *An optimal–order error estimate for the discontinuous Galerkin method,* Math. Comp., 50 (1988), pp. 75–88.

[17] W.H. Reed and T.R. Hill, *Triangular mesh methods for the neutron transport equation*, Technical Report LA-UR-73-479, Los Alamos Scientific Laboratory, Los Alamos, NM, 1973.

[18] Ch. Schwab, *p– and hp–Finite Element Methods. Theory and Applications to Solid and Fluid Mechanics,* Oxford University Press, Oxford, 1998.

[19] E. Süli, P. Houston and Ch. Schwab, *hp–Finite element methods for hyperbolic problems,* in The Mathematics of Finite Elements and Applications. MAFELAP X, J.R. Whiteman, ed., Elsevier, Oxford, 2000, pp. 143–162.

[20] E. Süli, Ch. Schwab and P. Houston, *hp–DGFEM for partial differential equations with nonnegative characteristic form,* in Discontinuous Galerkin Methods: Theory, Computation and Applications, B. Cockburn, G.E. Karniadakis and C.-W. Shu, eds., Lecture Notes in Computational Science and Engineering, Vol. 11, Springer, Berlin, 2000, pp. 221–230.